

# Non-Gaussian states produced by close-to-threshold optical parametric oscillators: role of classical and quantum fluctuations

V. D'Auria,<sup>1,\*</sup> C. de Lisio,<sup>2,3</sup> A. Porzio,<sup>4,†</sup> S. Solimeno,<sup>3,4</sup> Javaid Anwar,<sup>5</sup> and M. G. A. Paris<sup>6,7,8,‡</sup>

<sup>1</sup>*Lab. Kastler Brossel, Université Pierre et Marie Curie, Ecole Normale Supérieure, CNRS, 4 place Jussieu, 75252 Paris, France*

<sup>2</sup>*CRS Coherentia CNR-INFM, I-80126 Napoli, Italia.*

<sup>3</sup>*Dip. di Scienze Fisiche, Univ. "Federico II", Complesso Univ. Monte Sant'Angelo, I-80126 Napoli, Italia.*

<sup>4</sup>*CNISM UdR Napoli Università, I-80126 Napoli, Italia.*

<sup>5</sup>*Phys. Dept., COMSATS (CIIT) Islamabad, Pakistan.*

<sup>6</sup>*Dip. di Fisica, Università degli studi di Milano, I-10133 Milano, Italia.*

<sup>7</sup>*CNISM UdR Milano Università, I-20133 Milano, Italia.*

<sup>8</sup>*ISI Foundation, I-10133 Torino, Italia.*

Quantum states with non-Gaussian statistics generated by optical parametric oscillators (OPO) with fluctuating parameters are studied by means of the Kurtosis excess of the external field quadratures. The field generated is viewed as the response of a nonlinear device to the fluctuations of laser pump amplitude and frequency, crystal temperature and cavity detuning, in addition to quantum noise sources. The Kurtosis excess has been evaluated perturbatively up to the third order in the strength of the crystal nonlinear coupling factor and the second order in the classical fluctuating parameters. Applied to the device described in Opt. Expr. **13**, 948-956 (2005) the model has given values of the Kurtosis excess in good agreement with the measured ones.

PACS numbers: 42.65.Yj

## I. INTRODUCTION

Non Gaussian (NG) resources (*i.e.* NG states and/or operations) [1–6] are required for realizing relevant quantum information protocols, as for example entanglement distillation and swapping [7–10]. It has been demonstrated that they may improve the fidelity of teleportation [11–13] and cloning [14] and NG states are more effective in revealing nonlocality [15–18]. Thus the reliable generation of NG single- and two-mode states assumes a relevant role. Recently, few scheme to generate NG states based on conditional de-Gaussification protocols have been proposed [11–13] and realized [19, 20]. Moreover, it has been proven that phase diffusing a squeezed vacuum state makes it a NG ones [4–6].

Departures from Gaussian statistics have been observed (see Ref. [21]) in the outcomes for the field quadrature  $X_\theta = (e^{-i\theta}a + e^{i\theta}a^\dagger)/2$  outing a degenerate Optical Parametric Oscillator (OPO). These deviations have been quantified by measuring for different operating conditions the departure of the fourth moment  $\langle X_\theta^4 \rangle$  from its Gaussian value. In particular, it has been observed a dependence on the quadrature phase  $\theta$  with the maximum departure always appearing in correspondence of the anti-squeezed amplitude quadrature ( $\theta = 0$ ).

No doubt the observed deviations are due to a nonlinear response of the device to Gaussian quantum and classical fluctuating parameters, such as laser pump am-

plitude and phase, cavity length and OPO crystal temperature. While in the linear analysis only the quantum input noise contributes to the OPO output signal, by expanding the equation of motion to higher orders classical fluctuations contribute as well to the output. As a result of the multiplicative mixing of several noise sources, the signal loses its Gaussian character. The weight of these sources in determining the deviation from the Gaussian statistics was not clear at time of publication of Ref. [21]. The present paper is meant to present and discuss a consistent theoretical framework to explain and interpret the observed experimental evidences.

OPOs rely on parametric down-conversion: a strong *pump* beam at frequency  $\omega_p$  interacts in a non-linear crystal with the vacuum fields thus generating two beams, *signal* and *idler*, at frequencies  $\omega_s$  and  $\omega_i$  respectively [22–24]. This mechanism is represented in the Hamiltonian by the product of three field operators,  $a_p$  (pump),  $a_s$  (signal)  $a_i$  (idler) and described dynamically by Langevin equations. The model herein presented starts by including in the Graham and Haken Langevin Equations (GHLE) different classical noise sources. Then, expanding  $a_{s,i}$  as power series in the strengths of the quantum and classical fluctuations a hierarchy of Langevin equations is obtained in which the field at a given order acts as source for the next one. This has been done up to the third order thus culminating with Fig. 5 showing an adequate agreement of the computed difference (*Kurtosis excess*)  $K_\theta = (\langle X_\theta^4 \rangle - 3 \langle X_\theta^2 \rangle^2) / \langle X_\theta^2 \rangle^2$  with the measured values  $K_\theta$  of [21].

A perturbative analysis of an ideal OPO was already developed in [26]: according to it nonlinear contributions

\*Electronic address: virginia.dauria@spectro.jussieu.fr

†Electronic address: alberto.porzio@na.infn.it

‡Electronic address: matteo.paris@fisica.unimi.it

become comparable to the linear output only at a relative distance from the threshold of about  $\sim 10^{-6}$  while the data of Ref. [21] were measured at a distance of  $\sim 5 \times 10^{-2}$  so signalling the occurrence of more complex mechanisms. Hence, it has been essential to account for contributions from different fluctuating parameters each represented as a Gaussian process weighted by its standard deviations  $g_i$ . For the sake of generality the GHLE [25] model has been developed for a non degenerate OPO whereas the field moments have been calculated for a degenerate one so to allow a direct comparison with [21].

Different order fields have been represented as the convolution of the previous order one with a  $2 \times 2$  matrix  $\mathbf{G}$  which becomes singular on approaching the threshold. This singularity is at the origin of the enhancement of higher order effects in the critical region.

The paper is organized as follows. In Section II the extended GHLE model for an OPO with fluctuating parameters is introduced and discussed. The squeezing of the intracavity field is discussed in Sec. III. Section IV deals with the statistics of the quadratures outside the cavity as measured by a finite bandwidth detector. The deviation from the Gaussian statistics in terms of  $K_\theta$  is analyzed by dwelling on the agreement of the results provided by the model with the experimental findings. Plots of  $K_\theta$  vs.  $\theta$  and  $K_\theta$  for  $\theta = 0$  vs.  $E^2$  are reported. Section V closes the paper with concluding remarks. Details about the linearization, together with few analytical derivations are reported in the appendices.

## II. LANGEVIN EQUATIONS

Consider the set of the three OPO cavity modes  $a_k$  ( $a_p = e^{-i\omega_p t - i\phi_p} a_0$  pump mode at frequency  $\omega_p$  and phase  $\phi_p$ ,  $a_s = e^{-i\omega_s t - i\frac{1}{2}\phi_p} a_1$  and  $a_i = e^{-i\omega_i t - i\frac{1}{2}\phi_p} a_2$  respectively signal and idler modes with  $\omega_p = \omega_s + \omega_i$ ) whose mutual interaction under the action of a driving field  $e^{-i\omega_p t} \mathcal{E}$  is described by the Hamiltonian

$$H_{int} = i\hbar \frac{\chi}{2} (a_1 a_2 a_0^\dagger - a_0 a_1^\dagger a_2^\dagger) + i\hbar (\mathcal{E}^* a_0 - \mathcal{E} a_0^\dagger) \quad (1)$$

where  $\chi$  is the coupling parameter proportional to the crystal second order susceptibility  $\chi^{(2)}$ . Since real lasers are characterized by a field  $\mathcal{E} = \epsilon (1 + g_{\mu_p} \hat{\mu}_p) e^{-i\phi_p}$  of constant amplitude  $\epsilon$  modulated by a fluctuating factor  $1 + g_{\mu_p} \mu_p(t)$  ( $\langle \mu_p \rangle = 0$ ) times a phase factor  $e^{-i\phi_p}$ , where  $\phi_p(t)$  is a slowly diffusing phase, i.e.  $\langle (\phi_p(t) - \phi_p(t'))^2 \rangle = \Delta_\ell |t - t'|$  with  $\Delta_\ell$  the laser linewidth [24].

The cavity modes are characterized by damping factors  $\gamma_{k,M}, \gamma_{k,x}$  ( $\gamma_k = \gamma_{k,M} + \gamma_{k,x}$ ) due respectively to the output mirror ( $M$ ) and the other loss mechanisms (x: crystal absorption and scattering, absorption of the two mirrors, etc.). The evolution of the cavity mode operators can be described by the Graham-Haken Langevin equations

(GHLE) [25]:

$$\begin{aligned} \dot{a}_j &= - \left( \gamma_j - i\nu_j - i\frac{1}{2}\dot{\phi}_p \right) a_j + \frac{\chi}{2} a_0 a_j^\dagger \\ &\quad + e^{-ig_{\varpi_p} \phi_p/2} R_j \quad j = 1, 2 \text{ and } j \neq j' \\ \dot{a}_0 &= - \left( \gamma_0 - i\nu_0 - i\dot{\phi}_p \right) a_0 - \frac{\chi^*}{2} a_1 a_2 + \epsilon (1 + g_{\mu_p} \mu_p) \\ &\quad + e^{ig_{\varpi_p} \phi_p} R_0 \end{aligned} \quad (2)$$

where  $R_k(t) = \sqrt{2\gamma_{k,M}} b_{k,M} + \sqrt{2\gamma_{k,x}} b_{k,x}$  takes into account the delta correlated vacuum fluctuations,  $\langle b_{k,M,x}(t) b_{k,M,x}^\dagger(t') \rangle = \delta(t - t')$ , entering the OPO cavity. Modes are assumed to be slightly detuned by  $\nu_k = \frac{\pi c}{L_k} [L_k \frac{\omega_k}{\pi c}] - \omega_k$ , with  $L_k$  the OPO optical length at frequency  $\omega_k$  and  $[x]$  the closest integer to  $x$ .

In the following we will indicate by  $\kappa_k = \gamma_k - i\nu_k = |\kappa_k| e^{-i\psi_k}$  (with  $\psi_1 = \psi_2$ ) the complex damping coefficients, by  $\kappa = |\kappa_1 + \kappa_2|/2$  the mean decay rate and by  $\tau = \kappa t$  the time normalized to the cavity lifetime  $\kappa^{-1}$ . A caret will mark quantities normalized to  $\kappa$  (e.g.  $\hat{\epsilon} = \epsilon/\kappa$ ) and a tilde those such that the integral of their correlation function (e.g.  $\langle \hat{\mu}_p(\tau) \mu_p(\tau') \rangle = C_{\mu_p}(\tau - \tau')$ ) is equal to 1 (e.g.  $\int_{-\infty}^{\infty} C_{\mu_p}(\tau) d\tau = 1$ ). In particular the Gaussian delta-correlated process  $d\phi_p/dt$  will be replaced by  $d\phi_p/d\tau = g_{\varpi_p} \varpi_p$  with  $\langle \varpi_p(\tau) \varpi_p(\tau') \rangle = \delta(\tau - \tau')$  and  $g_{\varpi_p} = \sqrt[4]{\langle \hat{\Delta}_\ell^2 \rangle}$ .

In real devices, beside the fluctuations related to classical noise of the laser beam, the parameters  $\nu_k$  and  $\chi$  of Eqs. (2) experience also the effects of mechanical vibrations. Residual fluctuations of the cavity optical length  $\delta L_k$ , at frequency  $\omega_k$ , induce deviations  $\delta\nu_k = -(\delta L_k/L_k) \omega_k$  of the mode detunings from their average values  $\langle \nu_k \rangle$ . Usually, an active control guarantees that the standard deviation of  $\delta\nu_0$  is a small fraction of  $\gamma_0$ .

The parameter  $\chi$  is proportional to the crystal susceptibility  $\chi^{(2)}$  through the Boyd-Kogelnik function  $H_{BK}(\sigma, \varkappa, \xi)$  [27] of the phase-matching factor  $\sigma$ , the focusing parameter  $\xi$  and the crystal absorption  $\varkappa$ .  $\sigma(T)$  depends on the crystal temperature  $T$  through the refractive indices at the interaction wavelengths. If the cavity configuration is far from the concentric one the dependence of  $\xi$  on the cavity geometry fluctuations can be neglected. Under this assumption  $\chi$  will be replaced in the system (2) by  $\bar{\chi} e^{-i\phi_\chi} (1 + g_T \delta \hat{T})$  with  $\bar{\chi}$  depending on the slow variations of  $T$  while  $\phi_\chi$  is a phase depending on the position of the beam waist with respect to the crystal center. With an accurate alignment  $\phi_\chi$  can be set equal to 0.  $g_T$  is defined by:

$$g_T = \sqrt{\langle \delta T^2 \rangle} \frac{d \log H_{BK}}{dT}$$

In conclusion, the OPO analyzed in the following is characterized by four classical fluctuating parameters  $g_{\mu_p} \hat{\mu}_p, g_{\varpi_p} \varpi_p, g_{\nu_k} \delta \hat{\nu}$  and  $g_T \delta \hat{T}$ , where  $\hat{\mu}_p, \varpi_p, \delta \hat{\nu}$ , and

$\delta\hat{T}$  are Gaussian processes with unit standard deviations, and  $g_{\mu_p}, g_{\varpi_p}, g_{\nu_k} \left( = \frac{(\delta L_k/L_k) \omega_k}{(\delta L_0/L_0) \omega_0} g_{\nu_0} \right), g_T$  the corresponding weights. These four terms, together with  $g_\chi = |\bar{\chi}|/(2|\kappa_0\kappa|)^{1/2}$ , describing the non-linear interaction of strength  $\bar{\chi}$  [26], determine the OPO dynamics. For typical operating conditions, ( $g_\chi \simeq 10^{-6}$ ,  $\kappa \simeq 10 \div 20$  MHz,  $\sqrt{\langle \Delta_\ell^2 \rangle} \simeq 1 \div 1000$  Hz,  $\sqrt{\langle \delta T^2 \rangle} \simeq 1 \div 10$  mK, and  $\partial n/\partial T \approx 10^{-6} \div 10^{-4}$ )  $g_{\mu_p}, g_{\varpi_p}, g_{\nu_k}, g_T$  range in the respective intervals  $10^{-2} \div 10^{-1}, 10^{-4} \div 10^{-2}, 10^{-5} \div 10^{-1}, 10^{-5} \div 10^{-4}$ .

The extended GHLE system (2) may now be written as

$$\begin{aligned} \dot{a}_j &= - \left( \hat{\kappa}_j - i \frac{g_{\varpi_p} \varpi_p}{2} + i g_{\nu_j} \delta\hat{\nu} \right) a_j \\ &\quad + \sqrt{\frac{|\hat{\kappa}_0|}{2}} \left( 1 + g_T \delta\hat{T} \right) g_\chi a_0 a_j^\dagger \\ &\quad + e^{-i g_{\varpi_p} \phi_p/2} \hat{R}_j \\ \dot{a}_0 &= - \left( \hat{\kappa}_0 - i g_{\varpi_p} \varpi_p + i g_{\nu_0} \delta\hat{\nu} \right) a_0 \\ &\quad - \sqrt{\frac{|\hat{\kappa}_0|}{2}} \left( 1 + g_T \delta\hat{T} \right) g_\chi a_1 a_2 + \hat{\epsilon} (1 + g_{\mu_p} \hat{\mu}_p) \\ &\quad + e^{i g_{\varpi_p} \phi_p} \hat{R}_0 \end{aligned} \quad (3)$$

a dot indicating derivatives with respect to  $\tau$ .

The OPO admits a threshold value for the amplitude  $\epsilon = \epsilon^{th} = |\kappa_0| \sqrt{|\kappa_1 \kappa_2|} / (2|\bar{\chi}|)$ . Below threshold, the mode  $a_0$  has a non-zero mean value  $r_0$ , which is related to the driving field amplitude  $\hat{\epsilon}$  ( $\hat{\epsilon} = \hat{\kappa}_0 r_0$ ). Therefore separating the average part  $r_0$  from the fluctuating one  $\delta a_0 = r_0 \alpha_0$  we put  $a_0 = r_0 (1 + \alpha_0)$ , where  $\alpha_0 = \rho_0 - i\varphi_0$ . Conversely the modes  $a_j$  have zero mean value and will be expressed in terms of rescaled operators  $a_j = r_j \alpha_j$ , with the  $r_j$  defined in terms of  $r_0$

$$|\hat{\kappa}_j| r_j^2 = |\hat{\kappa}_0| r_0^2. \quad (4)$$

Passing now from the amplitudes  $a_k$  to the scaled quantities  $\alpha_k$ , the extended GHLE (3) is rewritten as:

$$\begin{aligned} \dot{\alpha}_j + \hat{\kappa}_j \alpha_j &= E |\hat{\kappa}_j| \alpha_j^\dagger + g_\chi \hat{N}_{\chi_j} \\ &\quad + |\hat{\kappa}_j| E \left( g_T \delta\hat{T} + \alpha_0 \right) \alpha_j^\dagger \\ &\quad + i \left( g_{\varpi_p} \varpi_p/2 - g_{\nu_j} \delta\hat{\nu} \right) \alpha_j \\ &\quad + |\hat{\kappa}_j| E g_T \delta\hat{T} \alpha_0 \alpha_j^\dagger, \\ \dot{\alpha}_0 + \hat{\kappa}_0 \alpha_0 &= - E |\hat{\kappa}_0| \alpha_1 \alpha_2 + g_\chi \hat{N}_{\chi_0} + \hat{\kappa}_0 g_{\mu_p} \hat{\mu}_p \\ &\quad + i g_{\varpi_p} \varpi_p - i g_{\nu_0} \delta\hat{\nu} + i g_{\varpi_p} \varpi_p \alpha_0 \\ &\quad - i g_{\nu_0} \delta\hat{\nu} \alpha_0 - E |\hat{\kappa}_0| g_T \delta\hat{T} \alpha_1 \alpha_2, \end{aligned} \quad (5)$$

where

$$E = \frac{g_\chi}{\sqrt{2\hat{\kappa}_0 \hat{\kappa}_1 \hat{\kappa}_2}} \hat{\epsilon} e^{i\psi_0} \quad (6)$$

The above equations describe the dynamics of the fluctuating fields  $\alpha_k$  as responses to the classical noise sources

$\hat{\mu}_p, \varpi_p, \delta\hat{\nu}, \delta\hat{T}$  and quantum terms

$$\begin{aligned} \hat{N}_{\chi_j} &= \hat{R}_j e^{-i g_{\varpi_p} \phi_p/2} / (g_\chi r_j) \\ \hat{N}_{\chi_0} &= \hat{R}_0 e^{i g_{\varpi_p} \phi_p} / (g_\chi r_0). \end{aligned}$$

The system (5) may be solved perturbatively upon expanding the field amplitudes as

$$\alpha_k = \sum_{m=1}^3 \alpha_k^{(m)}. \quad (7)$$

The first-order terms ( $m = 1$ ) correspond to the linearized system.  $\alpha_k^{(m \geq 2)}$  are generated by non linear sources  $s_k^{(m)}$  made of a quantum contribution, proportional to  $g_\chi^m$ , and of mixed terms involving products of quantum and classical fluctuations of the type  $g_\chi^{m-1} g_i$  and  $g_\chi^{m-2} g_i g_j$ . Any  $s_k^{(m)}$  involves fields calculated up to the  $(m-1)$ -th order. By substituting the  $\alpha_k$  expansion into (5) and grouping the terms corresponding to the same perturbative order, each  $\alpha_k^{(m)}$  can be calculated as the convolution of the components  $G_{kk'}$  of the Green's matrix (see Eq. (A1)) relative to the linearized system, with  $s_k^{(m)}$  and  $s_{k'}^{(m)\dagger}$ .

For a degenerate (the signal and idler fields collapse into a single field in this case) and tuned ( $\bar{\nu}_k = 0$ ) OPO the extended GHLE (5) reduces to

$$\begin{aligned} \dot{\alpha} + \hat{\kappa} \alpha &= E \alpha^\dagger + g_\chi \hat{N}_\chi + E \left( g_T \delta\hat{T} + \alpha_0 \right) \alpha^\dagger \\ &\quad + i \left( \frac{1}{2} g_{\varpi_p} \varpi_p - g_{\nu_j} \delta\hat{\nu} \right) \alpha + E g_T \delta\hat{T} \alpha_0 \alpha^\dagger \\ \dot{\alpha}_0 + \hat{\kappa}_0 \alpha_0 &= g_\chi \hat{N}_{\chi_0} + \hat{\kappa}_0 g_{\mu_p} \hat{\mu}_p + i g_{\varpi_p} \varpi_p - i g_{\nu_0} \delta\hat{\nu} \\ &\quad - \frac{E}{2} |\hat{\kappa}_0| \alpha^2 + i g_{\varpi_p} \varpi_p \alpha_0 - i g_{\nu_0} \delta\hat{\nu} \alpha_0 \\ &\quad - E |\hat{\kappa}_0| g_T \delta\hat{T} \alpha^2, \end{aligned} \quad (8)$$

where the parameter

$$E = \frac{2g_\chi}{\sqrt{2\hat{\kappa}_0}} \hat{\epsilon} = e^{i\psi_0/2} \frac{\hat{\epsilon}}{\hat{\epsilon}^{th}} = e^{i\psi_0/2} |E|$$

now represents the excitation  $\hat{\epsilon}$  normalized to the threshold  $\hat{\epsilon}^{th} = \sqrt{|\hat{\kappa}_0|}/2/g_\chi$  while  $\hat{N}_\chi(\tau)$ ,  $\hat{N}_{\chi_0}(\tau)$  and  $\varpi_p(\tau)$  are delta-correlated processes,

$$\begin{aligned} \langle \hat{N}_\chi(\tau) \hat{N}_\chi^\dagger(\tau') \rangle &= \frac{4}{|E|^2} \delta(\tau - \tau'), \\ \langle \hat{N}_{\chi_0}(\tau) \hat{N}_{\chi_0}^\dagger(\tau') \rangle &= \frac{4|\hat{\kappa}_0|^2}{|E|^2} \delta(\tau - \tau'), \end{aligned} \quad (9)$$

The correlation times for  $\hat{\mu}_p$  are typically of the order of  $0.2 \div 1 \mu s$ , while those for  $\delta\hat{\nu}$  and  $\delta\hat{T}$  are of the order of  $ms$  and  $s$  respectively. Although  $\delta\hat{\nu}$  and  $\delta\hat{T}$  can be treated adiabatically, we have preferred to treat the noise sources in a unified fashion.

### A. Nonlinear terms for a degenerate OPO

Expanding Eqs. (5) up to the third order the fields  $\alpha^{(m)}$  (signal=idler) and  $\alpha_0^{(m)}$  (pump) of (7), represented in the vector form  $\alpha^{(m)} = (\alpha^{(m)}, \alpha^{(m)\dagger})^T$ ,  $\alpha_0^{(m)} = (\alpha_0^{(m)}, \alpha_0^{(m)\dagger})^T$ , are given by

$$\alpha^{(m)} \int_0^t \mathbf{G}(t-\tau) \cdot \mathbf{s}^{(m)}(\tau) d\tau$$

$$\alpha_0^{(m)} \int_0^t \mathbf{G}_0(t-\tau) \cdot \mathbf{s}_0^{(m)}(\tau) d\tau$$

with  $\mathbf{G}$  and  $\mathbf{G}_0$  defined by Eq. (A2), while the signal  $\mathbf{s}^{(m)}$  and pump  $\mathbf{s}_0^{(m)}$  sources read respectively:

$$\begin{aligned} \mathbf{s}^{(1)}(\tau) &= g_\chi \mathbf{N}_\chi(\tau) \\ \mathbf{s}^{(2)}(\tau) &= \mathbf{B}^{(1)}(\tau) \cdot \alpha^{(1)}(\tau) \\ \mathbf{s}^{(3)}(\tau) &= B^{(2)} \alpha^{(1)\dagger}(\tau) \\ \int_0^\tau \left( g_\chi^2 \delta B^{(2)}(\tau - \tau') \mathbf{1} + \mathbf{B}^{(1,1)}(\tau - \tau') \right) \cdot \alpha^{(1)}(\tau') d\tau' \end{aligned} \quad (10)$$

and

$$\begin{aligned} \mathbf{s}_0^{(1)}(\tau) &= g_\chi \hat{\mathbf{N}}_{\chi 0}(\tau) + i [g_{\varpi_p} \varpi_p(\tau) - g_{\nu 0} \delta \hat{\nu}(\tau)] \mathbf{1}_- \\ &\quad + \kappa_0 g_{\mu_p} \hat{\mu}_p(\tau) \\ \mathbf{s}_0^{(2)}(\tau) &= i [g_{\varpi_p} \varpi_p \alpha_0 - i g_{\nu 0} \delta \hat{\nu} \alpha_0] \mathbf{1}_- - \frac{1}{2} E \kappa_0 \alpha^{(1)2} \end{aligned} \quad (11)$$

with  $\mathbf{1}_- = (1, -1)^T$  and  $\mathbf{B}^{(1)}$

$$\mathbf{B}^{(1)} = \begin{bmatrix} i \left( \frac{1}{2} g_{\varpi_p} \varpi_p - g_{\nu} \delta \hat{\nu} \right) & E \left( \alpha_0^{(1)} + g_T \delta \hat{T} \right) \\ E^* \left( P \alpha_0^{(1)\dagger} + g_T \delta \hat{T} \right) & -i \left( \frac{1}{2} g_{\varpi_p} \varpi_p - g_{\nu} \delta \hat{\nu} \right) \end{bmatrix}, \quad (12)$$

with  $P$  the permutation operator. Note that  $\delta \hat{T}$  and  $\alpha_0^{(1)}$  appear in the off-diagonal terms while  $\varpi_p$  and  $\delta \hat{\nu}$  are in the diagonal ones.

For a tuned OPO ( $\psi = \psi_0 = \phi_\chi = 0$ )  $B^{(2)}$ ,  $\delta B^{(2)}$  and  $\mathbf{B}^{(1,1)}$ , of Eq. (10-c), are given by

$$\begin{aligned} B^{(2)} &= E \langle \alpha_0^{(2)} \rangle = -\frac{g_\chi^2}{2(1-E^2)} - g_{\varpi_p} \frac{E}{\kappa_0} - g_\nu^2 \frac{E}{\kappa_0^2} \\ \delta B^{(2)}(\tau - \tau') &= -E^2 \kappa_0 G_0(\tau - \tau') \sigma_{\alpha\alpha^\dagger}^{(1,1)}(\tau - \tau') \\ \mathbf{B}^{(1,1)}(\tau - \tau') &= \langle \mathbf{B}^{(1)}(\tau) \cdot \mathbf{G}(\tau - \tau') \cdot \mathbf{B}^{(1)}(\tau') \rangle. \end{aligned}$$

with  $\sigma_{\alpha\alpha^\dagger}^{(1,1)}(\tau - \tau') = \langle \alpha^{(1)}(\tau) \alpha^{(1)\dagger}(\tau') \rangle$ . To be consistent with the above hierarchy, all moments  $\langle s^{(m)} s^{(m)} \rangle$  must satisfy the inequalities  $\langle s^{(1)} s^{(1)} \rangle > \langle s^{(2)} s^{(2)} \rangle > \langle s^{(3)} s^{(3)} \rangle$ . Close to the critical point,  $\langle s^{(1)} s^{(1)} \rangle$ ,  $\langle s^{(2)} s^{(2)} \rangle$  and  $\langle s^{(3)} s^{(3)} \rangle$  are of the order of  $O(g_\chi^2)$ ,  $O(g_\chi^2 g_i^2 (1-E)^{-1})$  and  $O(g_\chi^2 g_i^4 (1-E)^{-2})$  respectively, so that the above condition implies that the approximation maintains its validity up to  $1-E > g_i^2$ .

Since the linear source for the down-converted beam (see Eq. (10-a)) contains uniquely the quantum noise term, the effects of the classical fluctuations can be analyzed only going beyond the linear approximation.

### III. INTRACAVITY FIELD

The nonlinear contribution to the intracavity field is represented by the averaged tensor product with respect to the different fluctuating parameters  $g_i N_i$  ( $g_\chi N_\chi$ ,  $g_\chi N_{\chi 0}$ ,  $g_{\mu_p} \hat{\mu}_p$ ,  $g_{\varpi_p} \varpi_p$ ,  $g_\nu \delta \hat{\nu}$ , and  $g_T \delta \hat{T}$ ),

$$\begin{aligned} \sigma^{(NL)}(\tau) &= \langle \alpha(\tau) \alpha^T(0) \rangle - \langle \alpha^{(1)}(\tau) \alpha^{(1)T}(0) \rangle \\ &= \sigma^{(2,2)}(\tau) + \sigma^{(3,1)}(\tau) + \sigma^{(1,3)}(\tau) \\ &= g_\chi^2 \sum_i g_i^2 \sigma_i^{(NL)}(\tau) \end{aligned}$$

Relevant  $\sigma^{(m,n)}(\tau)$  are explicitly given by:

$$\begin{aligned} \sigma^{(2,2)}(\tau) &= \int_{-\infty}^\tau d\tau' \int_{-\infty}^0 d\tau'' \mathbf{G}(\tau - \tau') \cdot \langle \mathbf{B}^{(1)}(\tau') \cdot \sigma^{(1,1)}(\tau' - \tau'') \cdot \mathbf{B}^{(1)T}(\tau'') \rangle \cdot \mathbf{G}(-\tau'') \\ \sigma^{(3,1)}(\tau) &= \int_{-\infty}^0 d\tau \mathbf{G}(\tau - \tau') \cdot \left( B^{(2)} \begin{bmatrix} 0 & 1 \\ 1 & 0 \end{bmatrix} + \int_{-\infty}^\tau \left( \delta B^{(2)}(\tau - \tau') \mathbf{1} + \mathbf{B}^{(1,1)}(\tau - \tau') \right) \cdot \sigma^{(1,1)}(\tau') d\tau' \right) \end{aligned}$$

Of particular interest is the variance  $\langle X_{\pi/2}^{(NL)2} \rangle_l$  normalized to  $\langle X_{\pi/2}^2 \rangle$ , i.e. the weight, normalized to  $g_i^2$ , of

the nonlinear correction to the squeezed variance:

$$\begin{aligned} \lambda_i^{NL} &= \frac{\langle X_{\pi/2}^{(NL)2} \rangle_l}{\langle X_{\pi/2}^2 \rangle} \\ &= \frac{-\sigma_{\iota a a}^{(NL)}(0) + \sigma_{\iota a a^\dagger}^{(NL)}(0) + \sigma_{\iota a^\dagger a}^{(NL)}(0) - \sigma_{\iota a^\dagger a^\dagger}^{(NL)}(0)}{4 \langle X_{\pi/2}^2 \rangle} \end{aligned}$$

For a balanced and exactly tuned OPO we have

$$\begin{aligned}
\lambda_{\chi_0}^{NL} &= \frac{E(2E^3\hat{\kappa}_0 + 2E^2\hat{\kappa}_0(2 + \hat{\kappa}_0) + (2 + \hat{\kappa}_0)^2 - 2E(-2 + \hat{\kappa}_0(2 + \hat{\kappa}_0)))}{2(1 - E^2)(1 + E)(2 + \hat{\kappa}_0)(2 + 2E + \hat{\kappa}_0)}, \\
\lambda_{\phi_P}^{NL} &\simeq -\frac{\hat{\kappa}_0(2 + \hat{\kappa}_0) - E\hat{\kappa}_0(6 + \hat{\kappa}_0) + 2E^3(8 + 5\hat{\kappa}_0) - 2E^2(12 + \hat{\kappa}_0(9 + \hat{\kappa}_0))}{16(1 - E^2)\hat{\kappa}_0(2 + \hat{\kappa}_0)}, \\
\lambda_{\nu}^{NL} &\simeq -\frac{E(E^3 + 2\hat{\kappa}_0 - E^2(3 + \hat{\kappa}_0) - E(6 + \hat{\kappa}_0))}{2(1 - E^2)(1 + E)\hat{\kappa}_0^2}, \\
\lambda_T^{NL} &\simeq \frac{E^2(1 + E)^2 - (2 + E)(1 - E)\hat{\kappa}_0^2}{2(1 - E^2)(1 + E)\hat{\kappa}_0^2}, \\
\lambda_{\mu_P}^{NL} &\simeq \frac{2 + E^2}{2(1 + E)^2}.
\end{aligned} \tag{13}$$

As it is apparent from the above formulas the contribution of  $\hat{\mu}_p$  remains bounded on approaching the threshold ( $E \rightarrow 1$ ), whereas the other terms diverge as  $(1 - E)^{-1}$ , see Fig. 1.

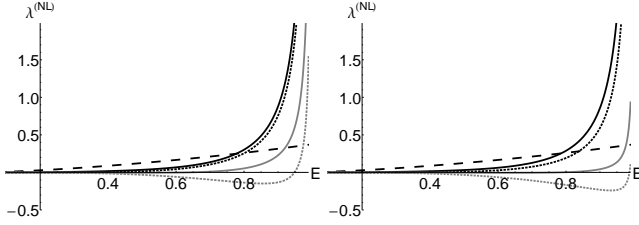


FIG. 1: Nonlinear contributions  $\lambda^{NL}$  (see Eqs. (13)) to intra-cavity squeezing, as functions of the normalized pump amplitude  $E$  for  $\hat{\kappa}_0 = 5$  (left) and  $\hat{\kappa}_0 = 10$  (right). In both plots:  $\lambda_{\chi}^{NL} \rightarrow$  black solid,  $\lambda_{\mu}^{NL} \rightarrow$  black dashed,  $\lambda_{\phi}^{NL} \rightarrow$  black dotted,  $\lambda_L^{NL} \rightarrow$  gray solid, and  $\lambda_T^{NL} \rightarrow$  gray dotted.

It is noteworthy that the ratio between  $\lambda_{\chi_0}^{NL}$  and the analogous quantity  $\lambda_{\chi_0}^{PPSE}$  calculated in [26] by means of the Positive P representation (PPSE) goes as  $\frac{\lambda_{\chi_0}^{NL}}{\lambda_{\chi_0}^{PPSE}} \simeq \frac{\hat{\kappa}_0 + 2}{3\hat{\kappa}_0 + 2} + O(1 - E)$ . In the limiting case of  $E \simeq 1$  the two approaches differ by a  $\hat{\kappa}_0$ -dependent factor bounded between 1/3 and 1. Such a substantial agreement between the two results in proximity of the singular point validates the use made in the present paper of the extended GHLE.

#### IV. KURTOSIS EXCESS AND COMPARISON WITH THE EXPERIMENTAL RESULTS

The field  $\alpha_{out,1}$  outing the OPO is a function of  $\alpha$ , the mirror damping coefficient  $\gamma_1$ , and the corresponding

input noise  $\mathbf{N}_1$  [29]

$$\alpha_{out,1} = g_{\chi} \sqrt{2\gamma_1} \left( \alpha - \frac{1}{2\hat{\gamma}_1} \mathbf{N}_1 \right). \tag{14}$$

Accordingly the generic output quadrature reads

$$X_{\theta} = \frac{1}{g_{\chi}^2 \sqrt{2\gamma_1}} \theta^T \cdot \alpha_{out,1} = X_{\theta}^{(1)} + X_{\theta}^{(2)} + \dots$$

where  $\theta = \frac{1}{2}(e^{-i\theta}, e^{i\theta})$  and  $X_{\theta}^{(m)}$  corresponds to  $\alpha^{(m)}$ . While  $X_{\theta}^{(1)}$  is Gaussian the terms  $X_{\theta}^{(m>1)}$  deviate from the normal distribution.

Quadratures are detected by a balanced homodyne and the relative current is measured by selecting a frequency  $\Omega_f$  and an integration time  $1/\hat{\gamma}_f$  [21, 30]. Accordingly, the detector output is represented by

$$V_{\theta} = \hat{F}_f X_{\theta} = \int_{-\infty}^0 e^{\hat{\gamma}_f \tau'} \cos(\Omega_f \tau') X_{\theta}(\tau') d\tau' \tag{15}$$

The deviation of  $V_{\theta}$  from a Gaussian distribution can be measured by the *Kurtosis-excess* parameter  $K_{\theta}$  (see Appendix D for details)

$$K_{\theta} = \frac{\langle : V_{\theta}^4 : \rangle - 3 \langle : V_{\theta}^2 : \rangle^2}{3 \langle : V_{\theta}^2 : \rangle^2} \simeq \sum_{\iota} g_{\iota}^2 \frac{\Upsilon_{\theta_{\iota}}}{\langle : V_{\theta}^{(1)2} : \rangle_{\chi}^2} \tag{16}$$

with  $\Upsilon_{\theta_{\iota}}$  given in Eq. (D1), the weight of the different noise sources indicated generally by  $N_{\iota}$ .

The spectral density  $\tilde{S}_{\mu_p}(w) = \langle \tilde{N}_{\mu_p}(-w) \tilde{N}_{\mu_p}(w) \rangle$  extends generally up to  $1 \div 2$  MHz. For the sake of simplicity it has been approximated by a uniform spectrum extending up to 1 MHz.  $\delta\tilde{\nu}$  and  $\delta\tilde{T}$  extend on very narrow bandwidths, while  $\tilde{N}_{\chi_0}$  and  $\tilde{\omega}_p$  are white noise sources.

In Fig. 2(a-d) we have plotted the five  $\Upsilon_{\iota}(\theta)$  vs.  $\theta$  for three excitation strengths  $E = 0.71, 0.87, 0.975$  of a

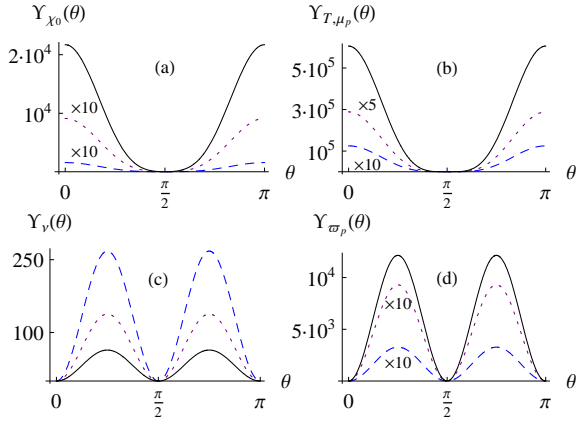


FIG. 2:  $\Upsilon_{\theta_i}$  (see Eq. (D1)) vs.  $\theta$  for different noise sources: (a) pump quantum noise; (b) amplitude and temperature; (c) cavity length; (d) pump phase. The plots, referred to different scaling factors, have been calculated for typical values of  $\Omega_f$  ( $= 0.3$ ),  $\gamma_f$  ( $= 0.15$ ) and  $E = 0.71$  (dashed blue),  $0.87$  (purple dotted),  $0.975$  (black).

perfectly tuned OPO with a pump cavity mode linewidth twice the signal one ( $\hat{\kappa}_0 = 2$ ), a condition similar to that of Ref.[21]. The graphs show that for  $N_{\chi_0}$ ,  $\hat{\mu}_p$ , and  $\delta\hat{T}$  the maximum deviation from a Gaussian appears for  $\theta = 0$ , while for  $\varpi_p$  and  $\delta\hat{\nu}$  it occurs for  $\theta = \pm\pi/4$ . (see Eq. (C2)).

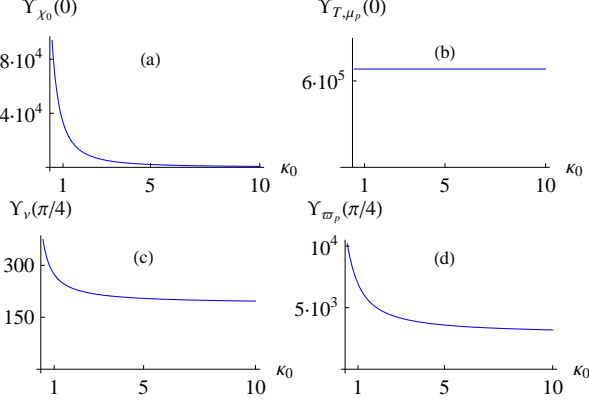


FIG. 3: Maxima of  $\Upsilon_{\theta_i}$  (see Eq. (D1)) vs.  $\kappa_0$  for the conditions of Fig. 2. ( $E \rightarrow 0.975$ ).

The maxima of  $\Upsilon_i(\theta)$  for  $N_{\chi_0}$ ,  $\varpi_p$  and  $\delta\hat{\nu}$  decrease for increasing  $\hat{\kappa}_0$  (see Fig. 3(a–d)). As expected from Eq. (12), the contribution of  $\delta\hat{T}$  is independent of  $\hat{\kappa}_0$ . The same holds true approximately for  $\hat{\mu}_p$  too having considered a technical noise bandwidth small compared to  $\hat{\kappa}_0$ .

Looking at Fig. 3 we see that the maximum for  $\Upsilon_{\mu_p,T}$  is at least one order of magnitude larger than the other ones. Moreover,  $g_{\mu_p} \gg g_T$  so that for pump level up to  $E^2 = 0.95$ , the NG behavior is essentially due to the laser amplitude fluctuations.

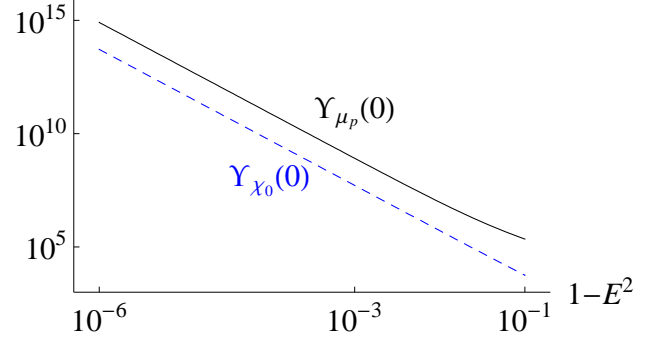


FIG. 4:  $\Upsilon_{0\chi_0}$  (pump quantum noise) and  $\Upsilon_{0\mu_p}$  (amplitude fluctuations) vs.  $1 - E^2$ .

In Fig. 4  $\Upsilon_{0\chi_0}$  (blue-dashed) and  $\Upsilon_{0\mu_p}$  (black-solid) are plotted vs.  $1 - E^2$  on a double logarithmic scale. Approaching the threshold the influence of  $N_{\chi_0}$  increases dramatically although  $\Upsilon_{0\chi_0}$  does not overcome  $\Upsilon_{0\mu_p}$ . Moreover,  $g_\chi \ll g_{\mu_p}$ , so that the observation of pure quantum effects, predicted by Drummond *et al.* [26], is demanded to future technology when either new materials with huge non-linear coefficients (enhanced  $g_\chi$ ) or very quiet lasers (reduced  $g_{\mu_p}$ ) will be available.

Being the laser amplitude noise the prominent source influencing the non-linear behavior we have compared some experimental findings of Ref. [21] with the predictions of the herein discussed model. In particular, the experimental behaviors of  $K_\theta$  and  $K_{\theta\mu_p}$  vs.  $\theta \in (-\pi, \pi)$  are reported in Fig. 5. Moreover, the maximum value of the experimental kurtosis, for  $\theta = 0$ , and  $g_{\mu_p}^2 \Upsilon_{0\mu_p}$  (see Eq. (16)) vs.  $E^2 \in (0.45, 0.97)$  are plotted in Fig. 6.

In general  $\Upsilon_{\theta\mu_p}$  can be represented by

$$\Upsilon_{\theta\mu_p} = \Upsilon_{4\mu_p} \cos 4\theta + \Upsilon_{2\mu_p} \cos 2\theta + \Upsilon_{0\mu_p} \quad (17)$$

with  $\Upsilon_{4,2,0\mu_p}$  functions of  $E, \hat{\kappa}_0$  and  $\hat{\kappa}$ . For very small deviations from the resonant configuration and  $|E|$  close to 1,  $\Upsilon_{\theta\mu_p}$  depends critically on  $|E|$

$$|E| = \frac{E_0}{\sqrt{\left(1 + 4\frac{\nu_p^2}{\gamma_s^2}\right) \left(1 + \frac{\nu_p^2}{\gamma_p^2}\right)}} \quad (18)$$

with  $E_0 = \epsilon|\bar{\chi}|/(\gamma_p\gamma_s^{3/2})$  the excitation strength at resonance.

The different heights of the peaks in the experimental data (see Fig. 5) can be ascribed to the variation of  $E$  during a measurement. The acquisition time for  $V_\theta$  for each  $\theta$  lasted about 2 ms, implying a total  $\theta$ -scanning acquisition time of 200 ms. The apparatus was equipped with a digital controller providing a crystal temperature time constant  $> 10^3$  s and a Drever-Pound system controlling the cavity tuning with a time constant  $> 10$  s. However, during the total acquisition time, slow drifts of the average cavity detuning  $\nu_p$  can occur thus inducing a

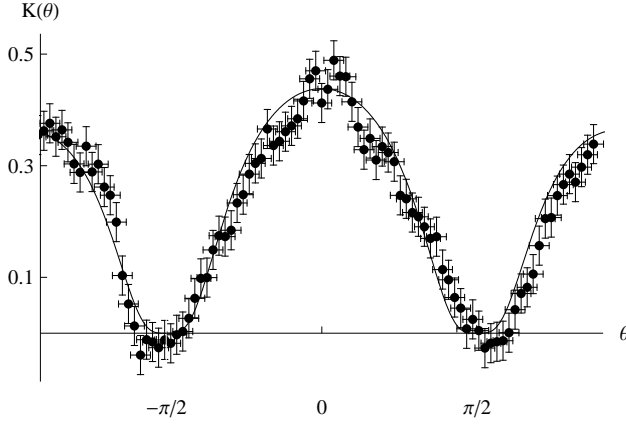


FIG. 5:  $K_{\mu_p}(\theta)$  (see Eq. (16)) overimposed to the experimental data of Ref. [21].  $K_{\mu_p}(\theta)$  has been calculated by assuming  $E^2 = 0.92$ ,  $\Omega_f = 0.3$ ,  $\gamma_f = 0.15$  and  $g_{\mu_p} = 0.007$ . The horizontal error bar accounts for the detector phase  $\theta$  stability, while the vertical one corresponds to the average spread between two neighbour  $K_\theta$  data.

variation of the effective excitation parameter  $E$  during the scan (see Eq. (18)). The simplest and more direct way to account for the time dependence of  $\nu_p$  is to set in (18)

$$\nu_p = \alpha(\theta - \theta_0) \quad (19)$$

with  $\alpha$  and  $\theta_0$  two fitting parameters and express the coefficients  $\Upsilon_{4,2,0\mu_p}$  in Eq. (17) as functions of  $\theta$ .

The best fit (continuous curve of Fig. 5) of the experimental data has been computed by assuming a spectral density  $\tilde{S}_{\mu_p}$  uniform in the interval  $0 \div 1.0$  MHz, in agreement with the laser (Lightwave mod. 142) technical noise specification and optimizing  $E_0$  (see (18)),  $\alpha$  and  $\theta_0$  (see (19)). The best agreement has been obtained for  $\alpha = 0.013$ ,  $\theta_0 = \pi$  and  $E_0 = 0.932$ , values corresponding to a drift of the resonance frequency of  $\approx 4\%$  the pump cavity mode linewidth and a variation of  $|E|$  of 0.006. Finally, normalizing  $g_{\mu_p}^2 \Upsilon_{\theta\mu_p}$  to the squared experimental variance (see Eq. (16)) the best agreement was obtained for  $g_{\mu_p} = 0.007$  in agreement with laser noise specification ( $< 1\%$ ).

The NG character depends critically on the distance from the threshold (see Fig. 4).  $g_{\mu_p}^2 \Upsilon_{0\mu_p}$  (see Eq. (16)) vs.  $E^2$  is compared to a set of 35 data obtained for five different values of  $E^2$  (0.5, 0.7, 0.8, 0.9, and 0.95) in Fig. 6. Plotted values have been obtained multiplying the experimental kurtosis by the relative squared variance. Error bars have been obtained by standard error propagation. The good agreement between the expected behavior and the data confirms, once more, the effectiveness of the model and the validity of assumptions about the relative noise strengths.

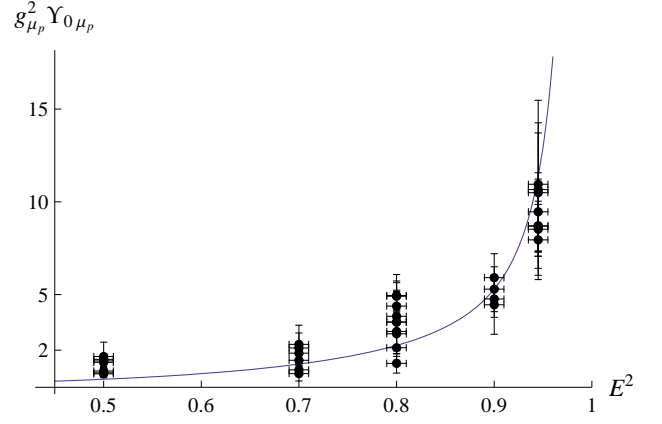


FIG. 6: Comparison of  $g_{\mu_p}^2 \Upsilon_{0\mu_p}$  (Eq. (16)) vs.  $E^2$  (solid curve;  $\Omega_f = 0.3$ ,  $\gamma_f = 0.15$  and  $g_{\mu_p} = 0.007$ ) with experimental data. Each experimental point has been obtained multiplying the measured kurtosis at  $\theta = 0$  for the relative squared variance. It is evident the agreement between data and theoretical curve within error bars.

## V. CONCLUSIONS

The statistical properties of the fields generated by an OPO depend on the fluctuations of many classical parameters, namely pump amplitude ( $g_{\mu_p} \hat{\mu}_p$ ), pump frequency ( $g_{\omega_p} \omega_p$ ), cavity detuning ( $g_\nu \delta \hat{\nu}$ ), and crystal temperature ( $g_T \delta \hat{T}$ ). In this paper it has been presented a model of the OPO based on an extension of the Graham-Haken quantum Langevin equations (GHLE) which accounts for the fluctuations of these parameters. The field generated has been dealt with as the response of a nonlinear device to these noise sources. Then, expanding the extended GHLE system at different orders in  $g_{\mu_p}$ ,  $g_{\omega_p}$ ,  $g_\nu$ ,  $g_T$  a hierarchy of equations has been obtained with  $\hat{\mu}_p$ ,  $\omega_p$ ,  $\delta \hat{\nu}$ ,  $\delta \hat{T}$  acting as noise sources together with the quantum noises ( $g_\chi \hat{N}_\chi$ ,  $g_{\chi_0} \hat{N}_{\chi_0}$ ) entering the optical cavity. These sources have been modeled as Gaussian processes with unit standard deviations weighted by the respective factors  $g_{\mu_p}$ ,  $g_{\omega_p}$ ,  $g_\nu$ ,  $g_T$  typically ranging in the intervals  $10^{-2} \div 10^{-1}$ ,  $10^{-7/2} \div 10^{-2}$ ,  $10^{-5} \div 10^{-1}$ ,  $10^{-5} \div 10^{-4}$ .

The extended GHLE solutions, obtained beyond the linear approximation, have been used for assessing the non-Gaussian character of the field outputting a degenerate OPO. The departure of the output quadrature  $X_\theta$  from the Gaussian statistics has been estimated by means of the *Kurtosis-excess* figure  $K_\theta = (\langle X_\theta^4 \rangle - 3 \langle X_\theta^2 \rangle^2) / \langle X_\theta^2 \rangle^2$ , i.e. the relative deviation of  $X_\theta$  4-th moment from the Gaussian expression of it. The model furnishes  $K_\theta$  as a sum of contributions from different parameters. Sets of plots have been provided, showing the dependence of  $K_\theta$  on the OPO operating condition, namely, the ratio pump/signal bandwidths, the excitation strength  $E$ , and the detection frequency  $\Omega_f$  and bandwidth  $\gamma_f$ . For typical operating conditions the pump technical noise emerges as the most critical factor.

The model has been used for reproducing the experimental values, reported in Ref. [21], of  $K_\theta$  vs.  $\theta$  and  $K_0$  vs.  $E^2$ . The good agreement, within the error bars, of the experimental data with the analytic predictions confirms the validity of the presented model. By providing a physically-insightful and computationally-effective parameterization of the OPO, the model may help in addressing the generation of non-Gaussian states by means of OPO sources.

### Appendix A: Linearization below threshold

The Fourier transform of the Green's functions  $\mathbf{G}, \mathbf{G}_0$  relative to a degenerate OPO are given by

$$\tilde{\mathbf{G}} = \frac{1}{\tilde{D}} \begin{bmatrix} \tilde{\Delta}^\dagger & e^{-i\vartheta} |E| \\ e^{i\vartheta} |E| & \tilde{\Delta} \end{bmatrix}, \quad \tilde{\mathbf{G}}_0 = \begin{bmatrix} \tilde{\Delta}_0^{-1} & 0 \\ 0 & \tilde{\Delta}_0^{\dagger-1} \end{bmatrix} \quad (\text{A1})$$

with  $\vartheta = \psi - \frac{1}{2}\psi_0$ ,  $\tilde{\Delta} = \hat{\kappa} - i\omega$ ,  $\tilde{D}(\omega) = \tilde{\Delta}\tilde{\Delta}^\dagger - |E|^2 = -(\omega + \omega_+)(\omega + \omega_-)$ ,  $\tilde{\Delta}_0 = \hat{\kappa}_0 - i\omega$ ,  $\omega_\pm = i \left( \cos \psi \mp \sqrt{|E|^2 - \sin^2 \psi} \right)$ . In particular for  $\hat{\kappa} = 1$  (tuned device) they correspond in the time domain to

$$\mathbf{G}(\tau) = \begin{cases} e^{-\tau} \begin{bmatrix} \cosh(E\tau) & \sinh(E\tau) \\ \sinh(E\tau) & \cosh(E\tau) \end{bmatrix} & \tau > 0 \\ 0 & \tau < 0 \end{cases}$$

$$\mathbf{G}_0(\tau) = \begin{cases} e^{-\hat{\kappa}_0\tau} \begin{bmatrix} 1 & 0 \\ 0 & 1 \end{bmatrix} & \tau > 0 \\ 0 & \tau < 0 \end{cases} \quad (\text{A2})$$

### Appendix B: Time-normal ordered correlation matrix : $\tilde{\sigma}^{(1,1)}(\omega)$ :

The Fourier transform :  $\tilde{\sigma}^{(1,1)}(\omega)$  : of the time-normal ordered matrix :  $\boldsymbol{\alpha}(\tau - \tau') := \langle \boldsymbol{\alpha}^{(1)}(\tau) \boldsymbol{\alpha}^{(1)T}(\tau') \rangle_\chi$  : (:  $\boldsymbol{\alpha}(\tau' - \tau) := \boldsymbol{\alpha}(\tau - \tau')$  : and :  $\boldsymbol{\alpha}_{a^\dagger a^\dagger} := \boldsymbol{\alpha}_{aa}^*$  :, :  $\boldsymbol{\alpha}_{aa^\dagger} := \boldsymbol{\alpha}_{a^\dagger a}$  :) is obtained from  $\tilde{\sigma}^{(1,1)}(\omega) = \tilde{\sigma}(\omega) / [(\omega^2 - \omega_+^2)(\omega^2 - \omega_-^2)]$  with

$$\tilde{\sigma}(\omega) = 4 \begin{bmatrix} \frac{\tilde{\Delta}^\dagger}{e^{-i\vartheta}|E|} & \frac{\tilde{\Delta}^\dagger(-\omega)\tilde{\Delta}(\omega)}{|E|^2} \\ 1 & \frac{\tilde{\Delta}}{e^{i\vartheta}|E|} \end{bmatrix}$$

by first normally ordering  $\tilde{\sigma}(\omega)$ ,

$$\tilde{\sigma}(\omega) \rightarrow \tilde{\sigma}_N(\omega) = 4 \begin{bmatrix} \frac{\tilde{\Delta}^\dagger}{e^{-i\vartheta}|E|} & 1 \\ 1 & \frac{(\tilde{\Delta}^\dagger)^*}{e^{i\vartheta}|E|} \end{bmatrix}$$

and then, symmetrizing with respect to time reversal

$$: \tilde{\sigma}^{(1,1)}(-\omega) := -\frac{2\omega_+}{\omega^2 - \omega_+^2} \tilde{\sigma}_N(-\omega_+) - \frac{2\omega_-}{\omega^2 - \omega_-^2} \tilde{\sigma}_N(-\omega_-)$$

$$= \frac{\tilde{\sigma}_{TN}(\omega)}{(\omega^2 - \omega_+^2)(\omega^2 - \omega_-^2)}$$

In particular for the tuned case

$$\tilde{\sigma}_{TN}(\omega) = 4 \begin{bmatrix} \frac{1+E^2+\omega^2}{2E} & 1 \\ 1 & \frac{1+E^2+\omega^2}{2E} \end{bmatrix} \quad (\text{B2})$$

### Appendix C: $\mathbf{B}^{(1)}$ expansion

The different noise sources  $N_i$  contribute to  $\tilde{\mathbf{B}}^{(1)}$  (Eq. (12)) through the terms:

$$\tilde{\mathbf{B}}^{(1)} = g_\chi \tilde{N}_{\chi_0} \tilde{\mathbf{B}}_\chi^{(1)} + g_\chi \tilde{N}_{\chi_0}^\dagger \tilde{\mathbf{B}}_\chi^{(1)T} + \sum_i g_i \tilde{N}_i \tilde{\mathbf{B}}_i^{(1)}, \quad (\text{C1})$$

with

$$\tilde{\mathbf{B}}_\chi^{(1)} = E \begin{bmatrix} 0 & \tilde{\Delta}_0^{-1} \\ 0 & 0 \end{bmatrix}$$

$$\tilde{\mathbf{B}}_{\mu_P}^{(1)} = \begin{bmatrix} 0 & e^{-i\vartheta} |E| \hat{\kappa}_0 \tilde{\Delta}_0^{-1} \\ e^{i\vartheta} |E| \hat{\kappa}_0^* \tilde{\Delta}_0^{\dagger-1} & 0 \end{bmatrix}$$

$$\tilde{\mathbf{B}}_{\omega_P}^{(1)} = i \begin{bmatrix} \frac{1}{2} & e^{-i\vartheta} |E| \tilde{\Delta}_0^{-1} \\ -e^{i\vartheta} |E| \tilde{\Delta}_0^{\dagger-1} & -\frac{1}{2} \end{bmatrix}$$

$$\tilde{\mathbf{B}}_T^{(1)} = \begin{bmatrix} 0 & e^{-i\vartheta} |E| \\ e^{i\vartheta} |E| & 0 \end{bmatrix}$$

$$\tilde{\mathbf{B}}_\nu^{(1)} = i \begin{bmatrix} -1 & e^{-i\vartheta} |E| \tilde{\Delta}_0^{-1} \\ -e^{i\vartheta} |E| \tilde{\Delta}_0^{\dagger-1} & 1 \end{bmatrix} \quad (\text{C2})$$

### Appendix D: Kurtosis-excess expansion

From the vanishing of the time-normal ordered correlations  $\langle : \alpha^{(1)} \mathbf{N}_1^T : \rangle = \langle : \alpha^{(2)} \mathbf{N}_1^T : \rangle = 0$ , it follows that:

$$\langle : X_\theta^{(l)} X_\theta^{(m)} : \rangle_\chi = \theta^T \cdot \langle : \alpha^{(l)} \alpha^{(m)T} : \rangle_\chi \cdot \theta$$

with  $l, m = 1, 2$ . Hence, retaining only the lowest non linear orders for  $\langle : V_\theta^4 : \rangle$  and  $\langle : V_\theta^2 : \rangle^2$ ,  $\Upsilon_{\theta_l}$  (see Eq. (16)) reads:

$$\Upsilon_{\theta_l} = \left\langle \left( \langle : V_\theta^{(1)} V_{\theta_l}^{(2)} + V_{\theta_l}^{(2)} V_\theta^{(1)} : \rangle_\chi \right)^2 \right\rangle_l$$

$$= \frac{1}{2\pi} \int_{-\infty}^{\infty} \tilde{S}_l(w) \theta^T \cdot \tilde{\zeta}_l(-w) \cdot \theta \theta^T \cdot \tilde{\zeta}_l(w) \cdot \theta dw$$

$$= \Upsilon_{4l} \cos 4\theta + \Upsilon_{2l} \cos 2\theta + \Upsilon_{0l} \quad (\text{D1})$$

with  $\tilde{S}_l(w) = \langle \tilde{N}_i(-w) \tilde{N}_i(w) \rangle$  and  $\tilde{\zeta}_l$  a  $2 \times 2$  matrix

$$\tilde{\zeta}_l(w) = (1 + \hat{T}) \left\langle : \left( \hat{F}_f \alpha_l^{(2)}(0) \right) \hat{F}_f \alpha^{(1)T}(0) : \right\rangle_\chi$$

$$= \frac{1}{2\pi} \frac{1}{\hat{\kappa}_0 - iw} \int_{-\infty}^{\infty} \tilde{H}(w, \omega) \tilde{\sigma}_l(w, \omega) d\omega, \quad (\text{D2})$$

$\hat{T}$  being a matrix transposition operator,  $\tilde{\sigma}_l(w, \omega)$  an entire function of  $\omega$  and  $w$

$$\tilde{\sigma}_l(w, \omega) = (1 + \hat{T}) (\hat{\kappa}_0 - iw) \tilde{D}(w + \omega) \tilde{\mathbf{G}}(w + \omega)$$

$$\cdot \tilde{\mathbf{B}}_l^{(1)}(w) \cdot \tilde{\sigma}_{TN}(\omega) \quad (\text{B1})$$



with  $\tilde{\sigma}_{TN}(\omega)$  defined in Eq. (B1),

$$\tilde{H}(w, \omega) = \frac{\tilde{F}_f(w + \omega) \tilde{F}_f(-\omega)}{\tilde{D}(w + \omega) (\omega^2 - \omega_+^2) (\omega^2 - \omega_-^2)}$$

and

$$\tilde{F}_f(\omega) = \frac{i}{2} \left( \frac{1}{\omega - \Omega_-} + \frac{1}{\omega - \Omega_+} \right)$$

the Fourier transform of  $\hat{F}_f$  (see Eq. (15)) while  $\Omega_{\pm} = \pm\Omega_f - i\gamma_f$ .

Since  $\lim_{|\omega| \rightarrow \infty} \omega \tilde{H}(w, \omega) \tilde{\sigma}_l(w, \omega) = 0$  the RHS of Eq. (D2) is given by the sum of residues

$$\tilde{\zeta}_l(w) = \frac{i}{\hat{\kappa}_0 - iw} \sum_{l=1}^4 H^{(l)}(w) \tilde{\sigma}_l(w, \omega_l) \quad (\text{D3})$$

where  $H^{(l)}(w) = \text{Res}_{\omega=\omega_l} [H(w, \omega)]$  for  $\omega_l = \omega_+, \omega_-, -\Omega_+, -\Omega_-$  ( $l = 1, 2, 3, 4$ ), poles of  $\tilde{H}(w, \omega)$  in the upper complex  $\omega$ -plane.

In the limiting case of zero centered delta-like sources  $\tilde{N}_i$  (see Eq. (C1))

$$\Upsilon_{\theta i} = \theta^T \cdot \tilde{\zeta}_i(0) \cdot \theta \theta^T \cdot \tilde{\zeta}_i(0) \cdot \theta$$

Such an approximation holds true for  $\tilde{N}_T, \tilde{N}_\nu$  and in a less measure for  $\tilde{N}_{\mu p}$ , depending on the laser technical

noise bandwidth normalized to the OPO cavity one. On the other extreme,  $\tilde{N}_{\chi_0}$  and  $\tilde{N}_{\varpi_p}$  represent white noises processes for which  $\Upsilon_{\theta\chi_0, \varpi_p}$  reduce to

$$\begin{aligned} \Upsilon_{\theta\chi_0, \varpi_p} &= - \sum_{l=1}^4 H^{(l)}(-i\hat{\kappa}_0) \\ &\quad \theta^T \cdot \sigma_{\chi_0, \varpi_p}(-i\hat{\kappa}_0, \omega_l) \cdot \theta \theta^T \cdot \tilde{\zeta}_{\chi_0, \varpi_p}(i\hat{\kappa}_0) \cdot \theta \\ &\quad - \sum_{l,i=1}^4 \frac{1}{\hat{\kappa}_0 + iw_i^{(l)}} \text{Res}_{w=-w_i^{(l)}} [H^{(l)}(w)] \\ &\quad \theta^T \cdot \tilde{\sigma}_{\chi_0, \varpi_p}(-w_i^{(l)}, \omega_l) \cdot \theta \theta^T \cdot \tilde{\zeta}_{\chi_0, \varpi_p}(w_i^{(l)}) \cdot \theta \end{aligned}$$

with  $\omega_l$  the frequencies of (D3) and  $w_i^{(l)}$  the poles of  $H^{(l)}(w)$  in the upper complex  $w$ -plane,

$$\begin{aligned} w_i^{(1)} &= \{2\omega_+, \omega_+ - \Omega_+, \omega_+ - \Omega_-, \omega_+ + \omega_-\} \\ w_i^{(2)} &= \{2\omega_-, \omega_- - \Omega_-, \omega_- - \Omega_+, \omega_- + \omega_+\} \\ w_i^{(3)} &= \{-2\Omega_+, \omega_+ - \Omega_+, \omega_- - \Omega_+, -\Omega_+ - \Omega_-\} \\ w_i^{(4)} &= \{-2\Omega_-, \omega_- - \Omega_-, \omega_+ - \Omega_-, -\Omega_- - \Omega_+\} \end{aligned}$$

- 
- [1] J. Eisert, S. Scheel, and M. B. Plenio, Phys. Rev. Lett. **89**, 137903 (2002);
  - [2] J. Fiurášek Phys. Rev. Lett. **89** 137904 (2002);
  - [3] D. E. Browne, J. Eisert, S. Scheel, M. B. Plenio, Phys. Rev. A **67**, 062320 (2003);
  - [4] A. Franzen, B. Hage, J. Di Guglielmo, J. Fiurášek, R. Schnabel, Phys. Rev. Lett. **97**, 150505 (2006);
  - [5] J. Fiurášek, P. Marek, R. Filip, and R. Schnabel, Phys. Rev. A **75**, 050302(R) (2007);
  - [6] T. Kiesel, W. Vogel, B. Hage, J. Di Guglielmo, A. Sambrowski, R. Schnabel, Phys. Rev. A **79**, 022122 (2009);
  - [7] C.H. Bennett, D.P. DiVincenzo, J.A. Smolin, and W.K. Wootters, Phys. Rev. A **54** 3824 (1996);
  - [8] J.-W. Pan, C. Simon, C. Brukner, A. Zeilinger, Nature **410** 1067 (2001);
  - [9] H. Aschauer and H.J. Briegel, Phys. Rev. Lett. **88** 047902 (2002); Phys. Rev. A **66**, 032302 (2002);
  - [10] Hiroki Takahashi, Jonas S. Neergaard-Nielsen, Makoto Takeuchi, Masahiro Takeoka, Kazuhiro Hayasaka, Akira Furusawa, Masahide Sasaki, "Non-Gaussian entanglement distillation for continuous variables", arXiv:0907.2159 (2009);
  - [11] T. Opatrny, G. Kurizki, and D.-G. Welsch, Phys. Rev. A **61**, 032302 (2000);
  - [12] P. T. Cochrane, T. C. Ralph, and G. J. Milburn, Phys. Rev. A **65**, 062306 (2002);
  - [13] S. Olivares, M.G.A. Paris, and R. Bonifacio, Phys. Rev. A **67**, 032314 (2003); S. Olivares, M. G. A. Paris, Las. Phys. **16**, 1533 (2006);
  - [14] N. J. Cerf, O. Krüger, P. Navez, R. F. Werner, and M. Wolf, Phys. Rev. Lett. **95**, 070501 (2005);
  - [15] S. Olivares, M. G. A. Paris, Phys. Rev. A **70**, 032112 (2004);
  - [16] S. Olivares, M. G. A. Paris, J. Opt. B **7**, S392 (2005);
  - [17] A. Ferraro, M. G. A. Paris, J. Opt. B, **7**, 174 (2005);
  - [18] C. Invernizzi, S. Olivares, M. G. A. Paris, K. Banaszek, Phys. Rev. A, Phys. Rev. A **72**, 042105 (2005);
  - [19] J. Wenger, R. Tualle-Brouiri, P. Grangier, Phys. Rev. Lett. **92**, 153601 (2004); A. Alexei Ourjoumtsev, R. Tualle-Brouiri, J. Laurat, and P. Grangier, Science **312**, 83 (2006); J. Heersink, Ch. Marquardt, R. Dong, R. Filip, S. Lorenz, G. Leuchs, and U. L. Andersen, Phys. Rev. Lett. **96**, 253601 (2006);
  - [20] A. Zavatta, S. Viciani, M. Bellini, Science **306**, 660 (2004);
  - [21] V. D'Auria, A. Chiummo, M. De Laurentis, A. Porzio, S. Solimeno, and M. G. A. Paris, Opt. Expr. **13**, 948 (2005); J. Řeháček, S. Olivares, D. Mogilevtsev, Z. Hradil, M. G. A. Paris, S. Fornaro, V. D'Auria, A. Porzio, and S. Solimeno, Phys. Rev. A **79**:032111 (2009);
  - [22] P. D. Drummond and P. Kinsler, Q. Opt. **7**, 727 (1995). P. Kinsler, P. D. Drummond, Phys. Rev. A **52**, 783 (1995);
  - [23] S. F. Pereira, Z. Y. Ou, H. J. Kimble, Phys. Rev. A **62**

- 042311 (2000);
- [24] M. D. Reid and P. D. Drummond, Phys. Rev. Lett. **60**, 2731 (1988); M. D. Reid and P. D. Drummond, Phys. Rev. A **40**, 4493 (1989); P. D. Drummond and M. D. Reid, Phys. Rev. A **41**, 3930 (1990);
  - [25] R. Graham and H. Haken, Z. Phys. **210**, 276 (1968); R. Graham, Z. Phys. **210**, 319 (1968);
  - [26] S. Chaturvedi, K. Dechoum and P. D. Drummond, Phys. Rev. A **65**, 033805 (2002); P. D. Drummond, K. Dechoum, S. Chaturvedi, Phys. Rev. A **65**, 033806 (2002); K. Dechoum, P. D. Drummond, S. Chaturvedi, M. D. Reid, Phys. Rev. A **70**, 053807 (2004);
  - [27] G. D. Boyd and D. A. Kleinman, J. Appl. Phys. **39**, 3597 (1968); Y. F. Chen and Y. C. Chen, Appl. Phys. B **76**, 645 (2003);
  - [28] S. Chaturvedi and P. D. Drummond, Eur. Phys. J. B. **8**, 251 (1999);
  - [29] M. J. Collett, C. W. Gardiner, Phys. Rev. A **30**, 1386 (1984); C. W. Gardiner, M. J. Collett, Phys. Rev. A **31**, 3761 (1985); M. J. Collett, D. F. Walls, Phys. Rev. A **32**, 2887 (1985);
  - [30] L. A. Wu, H.J. Kimble, J. L. Hall, and H. Wu, Phys. Rev. Lett. **57**, 2520 (1986).